CHEMBIOCHEM

DOI: 10.1002/cbic.200800473

Microfluidic Lithography to Create Dynamic Gradient SAM Surfaces for Spatio-temporal Control of Directed Cell Migration

Brian M. Lamb, Nathan P. Westcott, and Muhammad N. Yousaf*[a]

Cells exist in a complex, dynamic environment and are able to compute and process a myriad of signals, which initiate a range of diverse activities including cell growth, migration, and apoptosis.[1] Many extracellular signals are provided in either soluble or surface immobilized concentration gradients. Through these gradients, ligand- and receptor-mediated interactions cause the cell to generate local asymmetry, resulting in activation of signaling or cytoskeletal components. This in turn leads to changes in the sub-cellular nanoarchitecture and initiates a range of cellular behavioral responses.[2] In order to quantitatively and qualitatively understand the effects of surface-immobilized ligand gradients on development, directed migration (haptotaxis), inflammation, and wound healing, it is necessary to generate molecularly well-defined surface gradients integrated with dynamic surfaces for the spatial and temporal control of cell behavior.[1–3]

Although there are several strategies to generate switchable or dynamic surfaces for cell adhesion and migration, none are able to spatially and temporally control, at the molecular level, directed cell migration on dynamic gradients.[4] In order to quantitatively study the effects of surface immobilized ligand gradients on cell migration, the surface composition of the material should ideally meet the following criteria. The surface is 1) molecularly well defined, 2) inert to non-specific protein adsorption and cell adhesion, 3) compatible with a quantitative and chemoselective immobilization strategy to tether a variety of molecules to the surface, 4) enables dynamic, switchable control of surface composition at the molecular level, and 5) compatible with live-cell high-resolution fluorescence microscopy. We believe the most flexible surfaces to study biointerfacial phenomena are based on self-assembled monolayers (SAMs) of alkanethiolates on gold.[5] The synthetic flexibility of thiol chemistry with a variety of functional groups allows for a diverse set of orthogonal and chemoselective surface coupling strategies to be employed.[6] Furthermore, several techniques that provide high resolution spatial control[10–12] have been developed to pattern SAMs on gold, such as microcontact printing (μCP),[7] dip-pen nanolithography (DPN),[8] and photolithography.[9] Herein, we introduce a new strategy—microfluidic lithography (μFL)—to generate patterns and gradients of electroactive SAMs that can subsequently react chemoselectively to immobilize ligands[13] and can be dynamically controlled in the presence of cells to promote directional cell migration. We use these dynamic surfaces to show the migration of Swiss 3T3 fibroblasts towards the higher density regions of a biospecific cell adhesive peptide gradient. These gradients can be quantitatively characterized with both cyclic voltammetry (CV) and scanning electron microscopy (SEM), are straightforward to generate, and highly reproducible. This strategy can be generalized and used for a variety of biological studies in addition to its potential to pattern SAM gradients of any alkanethiol. μFL takes advantage of the intrinsic rapid rate of SAM formation of thiols on gold to create well-defined features and gradients.[14,15] We have shown previously that hydroquinone terminated SAMs are electroactive and provide both an activation method for ligand immobilization and a method to quantitate the density of ligands by in situ electrochemistry.

The oxidized quinone form is able to chemoselectively react with oxyamine-containing ligands to generate covalent, stable oxime linkages. This synthetic scheme is especially advantageous due to the ease of solid-phase peptide and carbohydrate synthesis of oxyamine-containing molecules and the commercial availability of oxyamine terminated ligands, monomers, and biomolecules. Furthermore, the interfacial oxime reaction to install ligands on the surface is fast, kinetically well-behaved, can be done at physiological conditions (37 °C, aqueous media) in the presence of cells, and does not cross react with proteins, nucleic acids, or other biopolymers.[15] Oxyamine-ligand immobilization on quinone SAMs can be analytically monitored with CV, which allows for precise measurement of the SAM surface composition. The strategy of μFL is illustrated in Figure 1. This is a straightforward, simple, and effective method to pattern micrometer-sized SAM features and can be utilized for the creation of hydroquinone-terminated SAM gradients. A polydimethylsiloxane (PDMS) microfluidic cassette is placed on the surface of a gold substrate, and a small volume of hydroquinone-terminated tetra(ethylene glycol) undecanethiol (H_2Q-TEG) solution is added to an access hole and slowly drawn into the microfluidic cassette through capillary action. The surface gradient is controlled by three parameters: 1) reactant depletion due to SAM formation on the gold surface as fluid flows through the channel, 2) differential surface exposure time due to the slow rate of capillary force driven fluid flow, and 3) thiol diffusion from the microfluidic channel into the PDMS cassette. By adjusting the thiol concentration and flow conditions with engineered patterns or syringe pumps, gradients of varying slopes can be produced. The gradient monolayer established by μFL is initially disordered and requires removal of the cassette and subsequent exposure to alkanethiol-containing solutions to backfill the remaining regions. For biological applications, these surfaces are immersed in 1 mM tetra(ethylene glycol) undecanethiol (TEG) in ethanol for 12 h.

[a] B. M. Lamb, N. P. Westcott, Prof. M. N. Yousaf
Department of Chemistry and the Carolina Center for Genome Science
University of North Carolina at Chapel Hill
Chapel Hill, NC 27599–3290 (USA)
Fax: (+1) 919-962-2388
E-mail: mnyousaf@email.unc.edu

Supporting information for this article is available on the WWW under http://www.chembiochem.org or from the author.

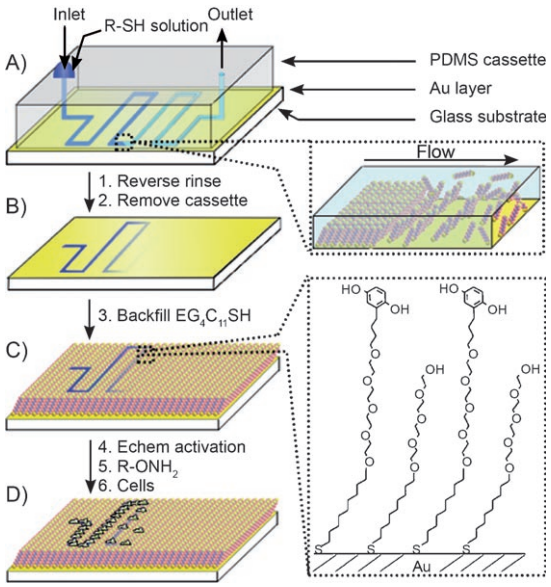

Figure 1. Schematic for creating an electroactive and chemoselective gradient SAM with microfluidic lithography. A) A PDMS microfluidic cassette is placed directly onto a bare gold surface. A solution of (0.2 mM H_2Q-TEG in EtOH, 30 s) is drawn through the microfluidic chamber and SAM formation occurs rapidly as fluid contacts surface. B) The PDMS cassette is reverse rinsed with EtOH then removed from the surface. C) The patterned gradient SAM surface is then placed in a 1 mM TEG solution for 12 h to backfill the remaining bare gold regions. D) Electrochemical oxidation converts the hydroquinone to the quinone and allows for subsequent chemoselective coupling to RGD-oxyamine peptides for biospecific cell adhesion and migration. Cells initially attach to the high density RGD regions and then proceed to migrate down the gradient until the RGD density no longer supports adhesion or migration.

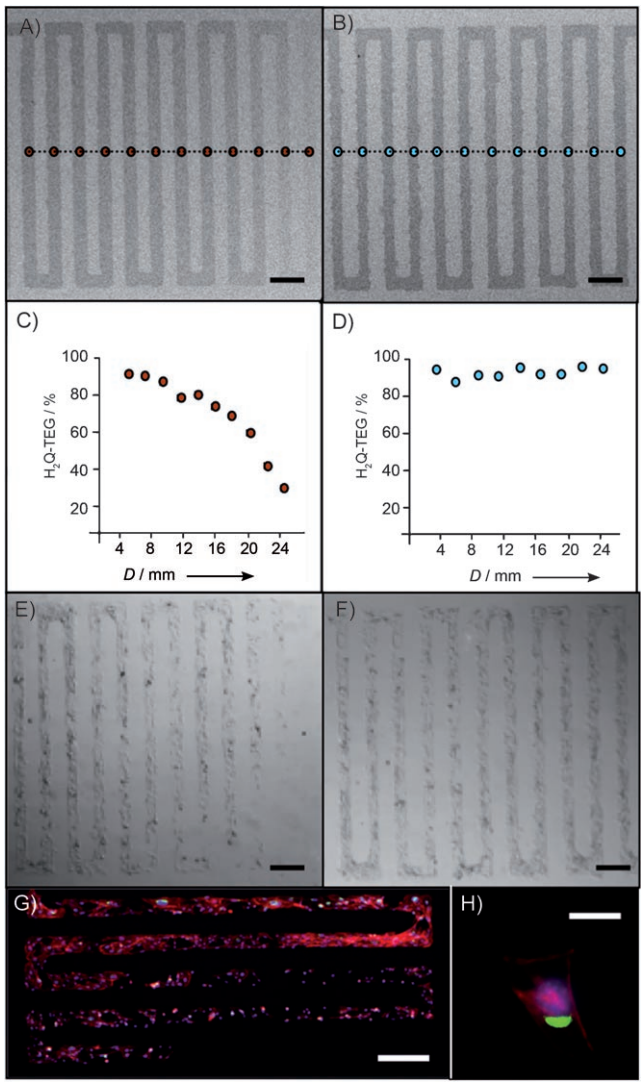

Figure 2. Characterization of electroactive gradients by scanning electron microscopy (SEM), electrochemistry and cell adhesion/migration. SEM image of a density gradient pattern (A) and constant density pattern (D) of H_2Q-TEG generated by microfluidic lithography. B) and E) Linescan intensity profiles of the gradient and constant density monolayers of figures (A, D), respectively. The plot tracks the density of H_2Q-TEG along the pattern. C) and F) Brightfield images of Swiss-Albino 3T3 fibroblasts adhered to RGD presenting surfaces. The cells proliferate and migrate to a minimum RGD density on the gradient substrate (C) but fill the constant density pattern (F) completely; (A–F: scale bar = 300 μm). G) On the gradient substrate cells were stained with fluorescent dyes to determine cell polarity at the limiting RGD density for adhesion and migration. The actin, nucleus and Golgi were stained and cells showed directional polarity towards the low density region; (scale bar = 300 μm). H) A single polarity stained cell, attached near the minimum RGD density to support cell attachment on the gradient (scale bar = 35 μm).

TEG serves to prevent nonspecific cell and protein adhesion and to fill the open sites that result from the rapid μFL-generated hydroquinone SAM gradient pattern.[16] To characterize the μFL-generated surfaces, the electroactive nature of the hydroquinone SAMs was used to precisely measure the amount (and therefore density) of redox active molecules present and subsequent ligand immobilization.[13] To visualize and quantify monolayer density on the gradient, SEM images of full (Figure 2A) and gradient (Figure 2D) hydroquinone monolayers were directly compared (Supporting Information) with electrochemical data. To correlate SEM images with electrochemical data, we generated a μFL pattern consisting of a full hydroquinone (100% surface coverage) monolayer (10 mM in EtOH, 60 s). We were able to show that these μFL conditions resulted in a full hydroquinone monolayer by calculating the density directly from the electrochemical data. For example, we used a μFL surface pattern of H_2Q-TEG with a surface area of 0.16 cm^2. To calculate H_2Q-TEG density we used the equation $Q = nFA\Gamma$ (Q represents total charge, n = mols of electrons (2), F = Faraday's constant, Γ = molecules per surface area). The theoretical surface density for a full electroactive monolayer should be approximately $\Gamma = 1.6 \times 10^{13}$ molecules with a total charge of Q = 5.1 μC. (We approximate a full monolayer coverage of 1×10^{14} molecules per cm^2 for H_2Q-TEG SAMs.) We experimentally determined a charge of 5.3 μC from the CV data, which closely approximates full monolayer coverage (5.1 μC) and demonstrates the rapid formation of microfluidic patterned SAMs. SEM images of the corresponding full monolayer pattern (100% H_2Q-TEG) are shown in Figure 2D. We used the same μFL procedure to generate varying densities of H_2Q-TEG patterns and characterized them using electrochemistry and SEM. From this data we were able to show that the amount (density) of hydroquinone in the pattern, which was determined precisely by electrochemistry, is directly proportional to the

corresponding pattern intensity from the SEM image. Linescan data points were obtained from SEM image files with Metamorph imaging software to quantitate hydroquinone density for the full (100%) monolayer and compared to the gradient monolayer. The gradient H_2Q-TEG pattern was generated by flowing 0.2 mM H_2Q-TEG in ethanol by using capillary action for 30 s. By comparing the linescan plots from the SEM data and pattern distance, an approximate measurement of the gradient H_2Q-TEG density could be determined (Figures 2B and E). It should be further noted that the flow of multiple different alkanethiols simultaneously and at different concentrations in the microfluidic cassette enables the rapid creation of complex but controlled patterned, mixed SAMs.

To show that patterns and gradients can be used for biospecific cell adhesion and migration, we electrochemically oxidized the surface to the quinone form and immobilized a cell-adhesive RGD-ONH_2 peptide. The RGD peptide is known to facilitate cell adhesion and migration through its specific interaction with cell surface integrin receptors.[17] Swiss Albino 3T3 fibroblasts were seeded to the surface for 3 h in serum-free media. For nongradient or uniform RGD patterns, cells adhered to the surface, and migrated and proliferated until the pattern was confluent (Figure 2F). For the gradient H_2Q-TEG pattern surfaces, cells initially adhered to the high density regions only and then slowly proliferated and migrated down the gradient until a minimal RGD density was reached that no longer supported adhesion, migration or growth; this density was determined to be 2×10^{12} molecules per cm^2 (Figure 2C). Cell polarity on the gradient surface was studied by staining cells for the Golgi, nucleus, and actin network. The vector that connects the nucleus centroid to the concentrated Golgi indicates directional polarity. Cells at the edge of the gradient are polarized towards the lower density of the gradient, but the analysis is complicated by competing cell–cell interactions and cell–material interactions. As controls, surfaces with no RGD immobilized or scrambled RDG immobilized showed no cell attachment, indicating that a biospecific interaction between cell surface integrin receptors and RGD ligands is required for adhesion and migration.[13] We next extended this strategy to generate dynamic surfaces for spatial and temporal control of directed cell migration. We wanted determine which direction cells would migrate after encountering a surface gradient. Haptotactic cell migration occurs on gradients of surface-bound biomolecules, but directional signals may be dynamically modulated or presented by factors such as trauma, gene up-regulation, transport of an internally held guidance molecule to tissue surfaces, or physico-mechanical forces.[18] To determine whether our μFL-patterned gradients would haptotactically direct cell migration to higher surface ligand densities, we combined two orthogonal patterning methodologies: 1) μCP to present hydrophobic sites for initial cell attachment and 2) μFL to produce gradients of hydroquinone that intersect with the microcontact printed features and can be dynamically controlled to present RGD peptides for directed cell migration (Figure 3). Bare gold surfaces were first microcontact printed with hexadecanethiols (HDT) to generate hydrophobic circles (500 μm diameter). An intersecting hydroquinone gradient was subsequently patterned using μFL. The hydroquinone SAMs remain latent until electrochemically activated and reacted chemoselectively to oxyamine functional groups. After installation of the hydroquinone gradient, the surface was then backfilled with tetra(ethylene)glycol alkanethiol (1 mM in ethanol) for 12 h to render it inert to nonspecific cell attachment. The surface was then exposed to fibronectin for 1 h to facilitate cell adhesion. Fibronectin only adsorbs to the microcontact printed circles. Application of an oxidative potential (750 mV for 10 s) converted the hydroquinone to the active quinone. Fibroblasts were seeded and only attached to the fibronectin containing circle patterns and became confluent by 24 h. The cell adhesive peptide RGD-ONH_2 (10 mM, 60 min) was then added and rapidly installed onto the quinone gradient. The advantage of the oxime reaction is that this reaction is fast, kinetically well behaved and can be done at physiological conditions without adverse side reactions.[13] After 2 h cells started to migrate from the circle and consistently migrated towards the high density region of the gradient. As a control, when no gradient (uniform RGD density) was μFL-patterned there was no bias in cell migration direction. These are the first results to show spatial and temporal control of cell migration on a biospecific cell adhesive gradient.

In summary, we have demonstrated a simple strategy for the creation of dynamic chemoselective gradients of SAMs with μFL for biospecific and directional cell migration studies. We have shown that these gradient patterns can be characterized quantitatively with SEM and CV. The incorporation of an orthogonal electroactive interfacial oxime reaction strategy allows for the ability to immobilize a wide variety of ligands to the μFL generated patterned gradients.[13,19] By combining μFL with μCP, spatial and temporal control of directional cell migration studies can be performed. Furthermore, the rapid formation of SAMs in microfluidic channels on gold surfaces can be advantageously utilized to create surface gradients of multiple functional alkanethiols. This technique is applicable to a wide variety of chemoselective and biologically relevant SAM systems, which may universally be characterized by SEM. Integrating this methodology with live-cell fluorescence microscopy will allow for numerous studies of cell behavior, including RNAi processing, cell migration, mitosis, and apoptosis.[20]

Experimental Section

Synthesis of alkanethiols: The undecane thiols terminated with tetra(ethylene glycol), and hydroquinone tera(ethylene glycol) were synthesized as reported previously.[13]

Solid-phase peptide synthesis: Peptide synthesis of RGDS-oxyamine was performed as previously reported.[10,13]

Electrochemistry: All electrochemical measurements were made by using a Bioanalytical Systems (West Lafayette, IN, USA) Epsilon potentiostat. An Ag/AgCl electrode served as the reference, the gold monolayer acted as the working electrode, and a Pt wire served as the counter electrode. The electrolyte was $HClO_4$ (1 M), and the scan rate was 100 $mV\,s^{-1}$. All measurements were made in a standard electrochemical cell.

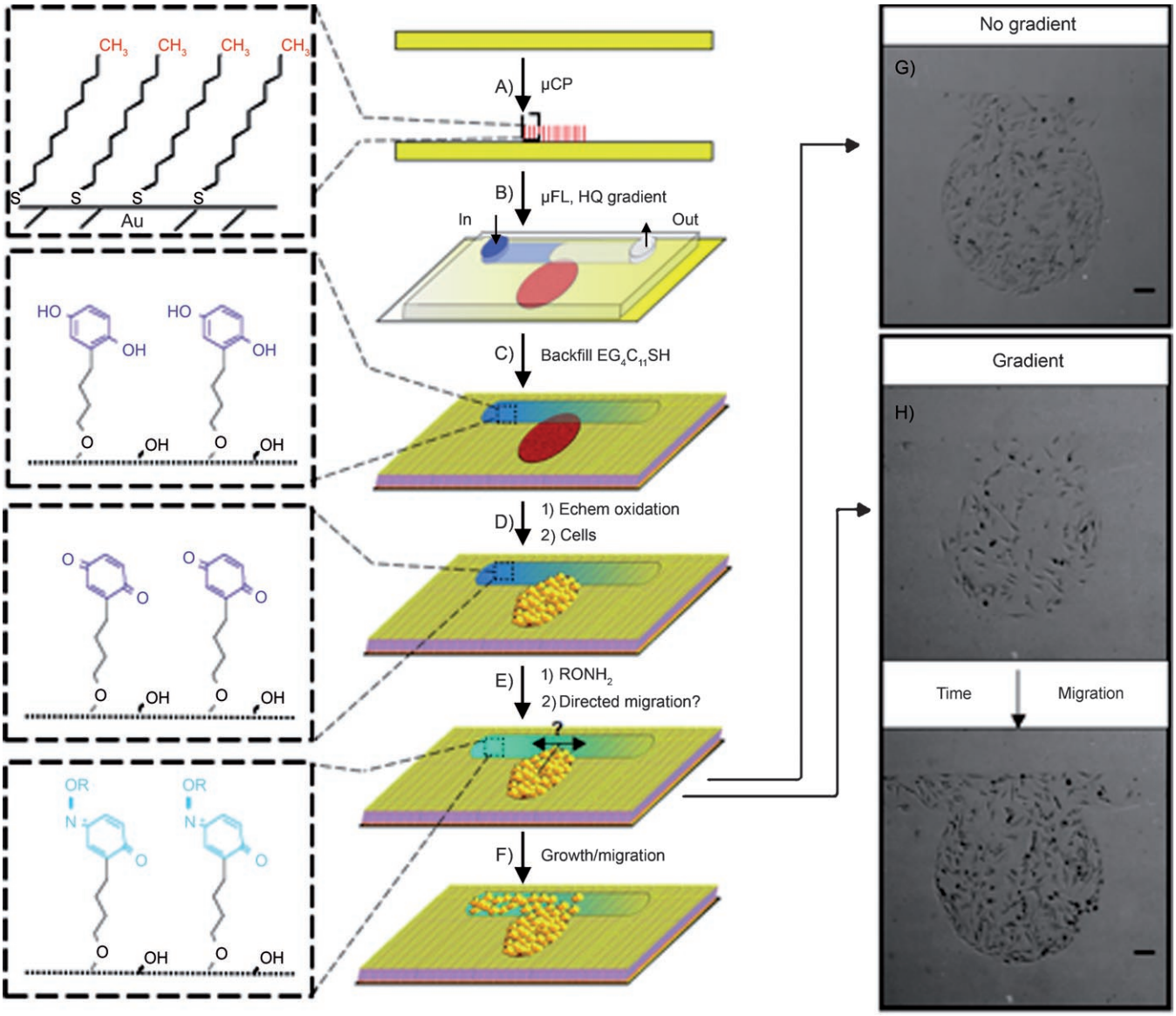

Figure 3. Combining microfluidic lithography generated gradients with microcontact printing to determine dynamic directed cell migration. A) Circles (500 μm diameter) of hexadecanethiol were microcontact printed μCP onto a gold surface (red). B) Intersecting these features, a H_2Q-TEG gradient was patterned utilizing μFL (blue). C) Removal of the PDMS cassette, and backfilling with TEG creates an ordered SAM surface. D) Electrochemical oxidation converts the hydroquinone to quinone on the patterned gradient region. Cells attached and proliferated and became confluent but remained confined to the HDT circle patterns. E) Addition of RGD-ONH_2 (10 mM, 60 min) installed the ligand onto the gradient quinone surface in the presence of cells. F) Cells proceeded to migrate from the circle patterns and encountered a gradient of biospecific RGD peptides providing a choice of directional migration. G) When a constant density of RGD is present the cells migrated in both directions equally with no bias in migration direction. H) On gradient RGD peptides, the cells consistently migrated toward the higher density of RGD peptides (up the gradient).

Microfabrication: The microchips were fabricated using soft lithography. Patterns were fabricated using masks drawn in Adobe Illustrator CS3 and photoplotted by Pageworks onto transparencies. The SU-8 50 (Microchem, Newton, MA, USA) was patterned by using the manufacturer's directions to obtain 100 μm channel depth with these masks. Slygard 184 (Dow Corning, Midland, MI, USA) was cast onto the mold in a 1:10 ratio (curing agent/elastomer, *w/w*). The prepolymer was degassed for 15 min and then poured over the mold. The prepolymer was cured for 1 h at 75 °C. The PDMS was removed from the master and access holes were punched into the PDMS to allow fluid flow.

Preparation of monolayers: Gold substrates were prepared by electron beam deposition of titanium (6 nm) and gold (24 nm) on 24×100 mm glass microscope slides. The slides were cut into 1× 2 cm^2 pieces and washed with absolute ethanol before use.

Microfluidic lithography (μFL): A 1 mM ethanolic solution of hydroquinone tetra(ethylene glycol) undecane thiol was flowed into the channels for 30 s to install a gradient SAM on the gold surface. The microfluidic cassette was then backflowed with ethanol for 10 s, PDMS cassette removed, and the remaining bare gold regions were backfilled with tetra(ethylene)glycol alkanethiol for 12 h.

For ligand density profiles: The SAM surfaces were oxidized at 750 mV for 15 s, then exposed to RGDS-ONH_2 (10 mM) for 3 h.

For dynamic experiments: A PDMS microfluidic cassette with a flow-restrictive pattern was used to slow capillary fluid flow. The μFL gradient of H_2Q-TEG thiol was patterned first (0.2 mM, 15 s flow), followed by μCP. The SAM surfaces were oxidized at 750 mV for 15 s and exposed to fibronectin (0.1 mg mL^{-1}) for 1 h. Cells were seeded overnight, then placed in 10 mM RGDS-ONH_2 solution for 1 h.

Oxyamine coupling reaction: The surface was activated with an application of 750 mV for 10 s to oxidize the hydroquinone to the reactive quinone. The surface was then exposed to the RGD-oxyamine peptide (10 mM, 3 h), and then rinsed thoroughly before cell seeding.

Cell culture: Swiss Albino 3T3 fibroblasts (ATCC) were cultured in Dulbecco's Modified Eagle Medium (Gibco) containing 10% calf bovine serum and 1% penicillin/streptomycin. Cells were removed with a solution of 0.05% trypsin in 0.53 mM EDTA , resuspended in serum-free medium (100000 cells per mL) for cell seeding, and allowed 2 h to attach to the surface prior to the addition of serum-containing media. For passage, cells were resuspended in the same 10 mL of medium that they were growing in, and 3 mL was transferred to 7 mL of fresh medium in a new flask.

Cell staining and visualization: Cell staining was done according to Hoover et al.[10] Phase-contrast and fluorescent images were taken using a Nikon Eclipse TE2000-E inverted microscope.

Scanning electron microscopy: Patterned SAMs were imaged on a Hitachi S-4700 Field Emission SEM and the intensity profile determined by Metamorph imaging software.

Acknowledgements

This work was supported by the Carolina Center for Cancer Nanotechnology Excellence and grants from the NIH to M.N.Y. and the Burroughs–Wellcome Foundation (Interface Career Award).

Keywords: cell migration · cell patterning · microfluidics · monolayers · redox chemistry

[1] K. Wong, H. T. Park, J. Y. Wu, Y. Rao, *Curr. Opin. Gen. Dev.* **2002**, *12*, 583–591.
[2] A. J. Ridley, M. A. Schwartz, K. Burridge, R. A. Firtel, M. H. Ginsberg, G. Borisy, J. T. Parsons, A. R. Horwitz, *Science* **2003**, *302*, 1704–1709.
[3] a) Y. Huang, X. Duan, Q. Wei, C. M. Lieber, *Science* **2001**, *291*, 630–633; b) J. Li, C. Papadopoulos, J. M. Xu, M. Moskovits, *Appl. Phys. Lett.* **1999**, *75*, 367–369; c) J-H. Kim, M. Yoneya, H. Yokoyama, *Nature* **2002**, *420*, 159–162; d) B. J. Scott, G. Wirnsberger, G. D. Stucky, *Chem. Mater.* **2001**, *13*, 3140–3150; e) J. Cembrero, A. Elmanouni, B. Hartiti, M. Mollar, B. Marí, *Thin Solid Films* **2004**, *451–452*, 198–202; f) X. Jiang, C. L. Jia, B. Szyszka, *Appl. Phys. Lett.* **2002**, *80*, 3090–3092.
[4] a) T. Okano, N. Yamada, M. Okuhara, H. Sakai, Y. Sakurai, *Biomaterials* **1995**, *16*, 297–304; b) W. S. Dillmore, M. N. Yousaf, M. Mrksich, *Langmuir* **2004**, *20*, 7223–7229; c) J. Nakanishi, Y. Kikichi, S. Inoue, K. Yamaguchi, T. Takarada, M. Maeda, *J. Am. Chem. Soc.* **2007**, *129*, 6694–6695; d) W. S. Yeo, C. D. Hodneland, M. Mrksich, *ChemBioChem* **2001**, *2*, 590–592; e) J. Genzer, R. R. Bhat, *Langmuir* **2008**, *24*, 2294–2317.
[5] a) M. N. Yousaf, B. T. Houseman, M. Mrksich, *Proc. Nat. Acad. Sci. USA* **2001**, *98*, 5992–5996; b) S. Petersen, J. M. Alonso, A. Specht, P. Duodu, M. Goeldner, A. del Campo, *Angew. Chem. Int. Ed.* **2008**, *47*, 3192–3195.
[6] J. C. Love, L. A. Estroff, J. K. Kriebel, R. G. Nuzzo, G. M. Whitesides, *Chem. Rev.* **2005**, *105*, 1103–1169.
[7] J. L. Wilbur, A. Kumar, H. A. Biebuyck, E. Kim, G. M. Whitesides, *Nanotechnology* **1996**, *7*, 452–457.
[8] R. D. Piner, J. Zhu, F. Xu, C. A. Mirkin, *Science* **1999**, *283*, 661–663.
[9] a) S. Petersen, J. M. Alonso, A. Specht, P. Duodu, M. Goeldner, A. Del Campo, *Angew. Chem. Int. Ed.* **2008**, *47*, 3192–3195; b) E. W. L. Chan, M. N. Yousaf, *Mol. BioSyst.* **2008**, *4*, 746–753.
[10] a) D. K. Hoover, E. W. L. Chan, M. N. Yousaf, *J. Am. Chem. Soc.* **2008**, *130*, 3280–3281; b) D. K. Hoover, E. J. Lee, E. W. L. Chan, M. N. Yousaf, *ChemBioChem* **2007**, *8*, 1920–1923.
[11] a) N. L. Jeon, S. K. W. Dertinger, D. T. Chiu, I. S. Choi, A. D. Stroock, G. M. Whitesides, *Langmuir* **2000**, *16*, 8311–8316; b) S. K. W. Dertinger, D. T. Chiu, N. L. Jeon, G. M. Whitesides, *Anal. Chem.* **2001**, *73*, 1240–1246.
[12] S. Morgenthaler, S. Lee, S. Zurcher, N. Spencer, *Langmuir* **2003**, *19*, 10459–10463.
[13] a) E. W. L. Chan, M. N. Yousaf, *J. Am. Chem. Soc.* **2006**, *128*, 15542–15546; b) E. W. L. Chan, M. N. Yousaf, *ChemPhysChem* **2007**, *8*, 1469–1472; c) E. W. L. Chan, S. Park, M. N. Yousaf, *Angew. Chem.* **2008**, *120*, 6363–6367; *Angew. Chem. Int. Ed.* **2008**, *47*, 6267–6271.
[14] A. Ulman, *Chem. Rev.* **1996**, *96*, 1533–1554.
[15] H.-G. Hong, W. Park, *Electrochim. Acta* **2005**, *51*, 579–587.
[16] C. Pale-Grosdemange, E. S. Simon, K. L. Prime, G. M. Whitesides, *J. Am. Chem. Soc.* **1991**, *113*, 12–20.
[17] M. D. Pierschbacher, E. Ruoslahti, *Nature* **1984**, *309*, 30–33.
[18] F. R. Zolessi, L. Poggi, C. J. Wilkinson, C.-B. Chien, W. A. Harris, *Neural. Dev.* **2006**, *1*, 2.
[19] a) S. Park, M. N. Yousaf, *Langmuir* **2008**, *24*, 6201–6207; b) B. M. Lamb, N. P. Westcott, M. N. Yousaf, *ChemBioChem* **2008**; DOI: DOI: 10.1002/cbic.200800400; c) B. M. Lamb, D. G. Barrett, N. P. Westcott, M. N. Yousaf, *Langmuir* **2008**, *24*, 8885–8889.
[20] a) E. W. L. Chan, M. N. Yousaf, *Angew. Chem.* **2007**, *119*, 3955–3958; *Angew. Chem. Int. Ed.* **2007**, *46*, 3881–3884; b) D. G. Barrett, M. N. Yousaf, *Angew. Chem. Int. Ed.* **2007**, *46*, 7437–7439; c) L. Hodgson, E. W. L. Chan, K. M. Hahn, M. N. Yousaf, *J. Am. Chem. Soc.* **2007**, *129*, 9264–9265.

Received: July 10, 2008
Published online on September 26, 2008

